

Deep Active Visual Attention for Real-time Robot Motion Generation: Emergence of Tool-body Assimilation and Adaptive Tool-use

Hyogo Hiruma¹, Hiroshi Ito^{1,2}, Hiroki Mori³, and Tetsuya Ogata^{1,4}

Abstract—Sufficiently perceiving the environment is a critical factor in robot motion generation. Although the introduction of deep visual processing models have contributed in extending this ability, existing methods lack in the ability to actively modify what to perceive; humans perform internally during visual cognitive processes. This paper addresses the issue by proposing a novel robot motion generation model, inspired by a human cognitive structure. The model incorporates a state-driven active top-down visual attention module, which acquires attentions that can actively change targets based on task states. We term such attentions as role-based attentions, since the acquired attention directed to targets that shared a coherent role throughout the motion. The model was trained on a robot tool-use task, in which the role-based attentions perceived the robot grippers and tool as identical end-effectors, during object picking and object dragging motions respectively. This is analogous to a biological phenomenon called tool-body assimilation, in which one regards a handled tool as an extension of one's body. The results suggested an improvement of flexibility in model's visual perception, which sustained stable attention and motion even if it was provided with untrained tools or exposed to experimenter's distractions.

Index Terms—Neurorobotics, Bioinspired robot learning, Visual Attention Mechanism, Imitation learning

I. INTRODUCTION

UNDERSTANDING the relationship between the body and environment is an essential task for both robots and humans, in order to accurately predict the results of a motion. Humans associate the relationships, or body schema, through body babbling and dynamic touches [1], both of which infants perform to empirically verify the link between vision, haptics, and self produced motions.

In robot task learning, conventional rule-based methods used manually pre-programmed relationships which generate precise motions, but were only applicable to strictly controlled

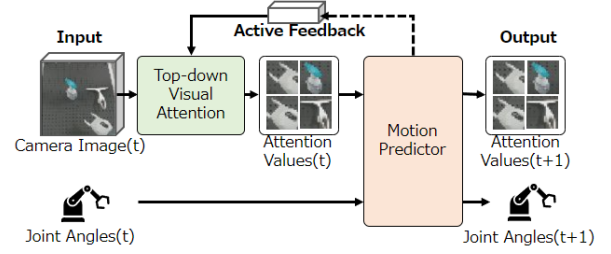


Fig. 1. Abstract structure of the proposed motion generation model. The top-down visual attention module extracts informative visual data from camera image based on active feedback of the succeeding motion predictor module.

environments. Conversely, learning-based methods acquire relationships by learning through interactions of trial and error [2], [3], imitating demonstrated motions [4], [5], or motor babbling [6], which is inspired by human's body babbling behaviours. In particular, end-to-end learning methods [6], [7], [8] directly associated visual and motor sensory data as body schema, which induced vision modules to selectively extract image data that are task-relevant. However, the environment modeled by such vision modules tended to be biased by the training data, which failed to adapt to recognize environment at untrained situations. Since the construction of body schemata strongly depends on visual information, such a lack of adaptability induces distorted environment recognition.

The visual perception of humans utilizes a cognitive structure called visual attention [9], [10], which selectively extracts information from attended local visual area. Human visual attention is an integrated system of bottom-up (passive) attention and top-down (active) attention. The former passively collects conspicuous visual patterns, whereas the latter actively filters out the collected stimuli to acquire the desired information. The desired information are selected based on what is held in one's working memory. Since the active attention enables self-control of the visual perception targets, humans are capable of attending to appropriate targets based on different situations. We consider that such "activeness", which existing robot vision models lack, enables humans to efficiently model environments with less biased recognition.

This paper proposes a novel real-time robot motion generation model, as shown in Fig. 1, inspired by human cognitive structures. The model is composed of a top-down attention module and a motion predictor module, in which the internal states of the latter module are constantly fed back to actively modify attention targets. The model was trained on a robot tool use task, which acquired role-based attentions in contrast

Manuscript received: February, 24, 2022; Revised May, 27, 2022; Accepted June, 22, 2022. This paper was recommended for publication by Editor A. Banerjee upon evaluation of the Associate Editor and Reviewers' comments. This work was supported by Hitachi, Ltd.

¹Hyogo Hiruma, Hiroshi Ito and Tetsuya Ogata are with the Department of Intermedia Art and Science, Waseda University, Tokyo, Japan hiruma@idr.ias.sci.waseda.ac.jp, hiroshi.ito.ws@hitachi.com, ogata@waseda.jp

²Hiroshi Ito is with the Center for Technology Innovation - Controls and Robotics, Research & Development Group, Hitachi, Ltd., Ibaraki, Japan

³Hiroki Mori is with the Future Robotics Organization, Waseda University, Tokyo, Japan mori@idr.ias.sci.waseda.ac.jp

⁴Tetsuya Ogata is with the Waseda Research Institute for Science and Engineering (WISE) at Waseda University, and the National Institute of Advanced Industrial Science and Technology (AIST), Tokyo, Japan

Digital Object Identifier (DOI): see top of this page.

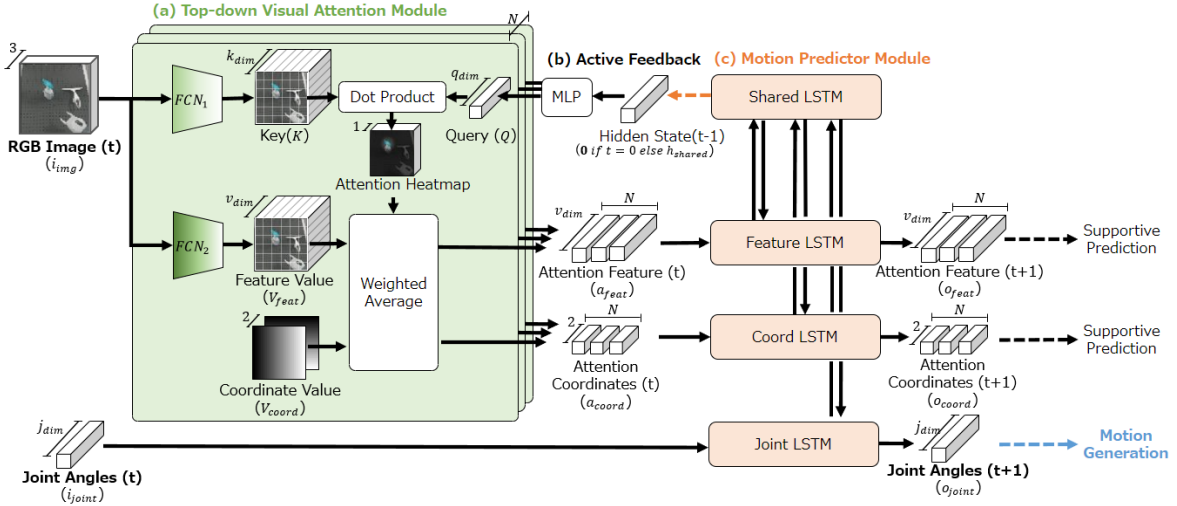


Fig. 2. Detailed structure of the proposed model: (a) Top-down visual attention module, (b) Active feedback connection and (c) Motion predictor module. The attention module selects and extracts feature and coordinate values at multiple visual attention points and the motion module uses them along with current robot joint angle values, for predicting each future values. Via active feedback, the attention targets are constantly updated based on the internal states of the motion module.

to conventional appearance-based attentions. The attention indicated visual recognition similar to Japanese macaques, suggesting an emergence of a biological phenomenon called tool-body assimilation.

II. RELATED WORK

A. Visual perception in robot control

In robot tasks, camera images are commonly utilized as the main source for perceiving the environment. However, as raw pixel data include irrelevant noises, directly using image data leads to a distorted perception, which negatively affects the construction of the robot's body schema.

Various vision processing models have been proposed to extract informative data from camera images, such as rule-based saliency maps [11]. Studies have proposed learning-based vision models that solely learn object-centric representations [12], [13] to explicitly extract data of certain objects. By contrast, end-to-end learned models jointly train vision models along with robot control models. This makes the vision models, such as widely used vanilla fully convolutional networks (FCN), to extract task-oriented features even from untrained objects [7], [14], [8]. However, FCNs lack in spatial generalization ability [15], and cannot extract data at untrained visual areas. Although training with large dataset can mitigate such inability, the data collection cost is a large burden especially; this is a common issue when employing other visual attention models such as vision transformers [16], [17].

Recent visual attention models specialized for robots [8], [18], [19] achieved high spatial generalizability with data efficiency, by employing a structure that explicitly extracts coordinate values of the predicted visual attention points. However, the inherent structure which assumes the attention targets to have consistent appearances removed the ability to generalize to untrained objects. While some models enabled top-down control of attention targets based on human inputs [20], [21], they cannot perform on site self-controlling which is to direct to necessary targets based on current motion states.

The proposed model adds “activeness”, as in humans, to self-control the attention targets, by providing motion prediction feedback to the visual attention module. We term our model as “Active” in contrast to other existing “Passive” attention models.

B. Tool-use learning

How one perceives a tool is an important metric when evaluating how it recognizes the relation between itself and the environment. Tool use behaviors are exhibited by animals to overcome their physical limitations. Animals show high dexterity by perceiving the tool as if it is a part of their bodies [22], [23]. Iriki et al. [22] suggested that Japanese macaques perceived the tool as an extension of their body after being trained to use them (tool-body assimilation). Specifically, such assimilation did not occur when macaques “held” the tool. Rather, it occurred when they were trained to “use” the tools. This suggests that actively perceiving to associate bodies, objects, and environments is essential to efficiently learn to use unaccustomed tools. Accordingly, how one recognizes the tool indicates how flexibly one can redefine the body schema.

Given the flexible tool-use behaviours of humans, previous studies of robot tool-use [6], [24], [25] proposed methods that enable the robots to control different tools in a single model, by predicting tool inertia parameters. The parameters were predicted by tool-held motor babbling [6], computing from the observed force and torques when swinging tools [24], and exploratory behaviours [25], which enabled the model to generalize to handle untrained tools. However, as the parameters cannot be predicted on the fly, the models cannot predict motions that requires to automatically switch tools based on transitioning situations. This suggests the lack in capability to redefine the body schema in real-time. Therefore, this research focuses to verify the flexible recognition of the proposed method, by evaluating whether it holds the capacity to redefine the body schema without specialized training methods for tool-body assimilation.

III. PROPOSED METHOD

A. Design concept

The proposed model is a robot motion generation model which actively modifies what to perceive in a task-state-driven and top-down manner (Fig. 2). The inputs are image data i_{img}^t and robot joint angle data i_{joint}^t at time step t , and the output is the prediction of next joint angles o_{joint}^{t+1} . The model generates robot motions by repeating the sequence of predicting the next joint angles and applying them to the robot [7], [14], [8].

The model consists of a top-down visual attention module (Fig. 2 (a)) and a motion predictor module (Fig. 2 (c)) which are connected with a forward pass and an active feedback (Fig. 2 (b)). The visual attention module is based on our previous “Passive” top-down attention model [20], but is extended to preform “Active” on site target control, by the whole structure of this model. This paper distinguishes “Active” and “Passive” attention by whether the model self-controls the attention via temporal internal feedbacks, or is controlled via external inputs, respectively; models that do not incorporate top-down information is also considered “Passive” (e.g. self-attention). The motion predictor module is composed of a “Layered” Long-Short Term Memory (LSTM) structure which is inspired by [26], in contrast to existing models that output visuomotor predictions with a “Single” LSTM. This structure enables higher and lower layered LSTMs to predict transitions of abstract task states and raw modality data respectively. Especially, separating the abstract transition is beneficial for creating active feedbacks that reflect slowly transitioning task states instead of rapidly changing raw modality values.

The structures of this model are inspired by human cognitive structures. The active feedback connection of the two modules is analogous to human visual attention, which controls attention targets based on information that are held in the working memory. The motion predictor module plays the role of the working memory. It is also designed to mimic the function of human working memory which simultaneously possess both integrated (abstract) and unintegrated (raw) data of different modalities, or stimuli [27].

B. Top-down visual attention module

This module (Fig. 2(a)) predicts task-relevant visual areas and selectively extracts the corresponding feature and coordinate values [20]. The module generates key-query-value representations, which is trained to extract information that are task-relevant. The key K is an image feature of input i_{img} , and the query Q is a vector that represents the feature of attention targets. The value consists of two representations: the feature value V_{feat} and coordinate value V_{coord} . The former is an image feature of the input i_{img} , and the latter is an absolute position embedding of Cartesian coordinates. This model converts attention maps to coordinate and feature values to effectively compress the data for the succeeding motion prediction and to perform object spatial recognition with high data-efficiency, as described in [20].

The attention is computed in two phases. The first phase generates an attention heatmap M through the scaled channel-wise dot product of K and Q , followed by a spatial softmax

function. The heatmap places high values at pixels of K that contain features similar to vector Q , which indicate the existence of an attention target. The second phase computes a weighted average of V_{feat} and V_{coord} in spatial dimensions by utilizing M as the weight of each pixel. This selectively extracts values at attention-target pixels: a_{feat} and a_{coord} .

$$M = Softmax_{2D} \left(\frac{K \odot Q}{\sqrt{HW}} \right) \quad (1)$$

$$a_{feat} = \sum_{u=0}^W \sum_{v=0}^H M_{(u,v)} V_{feat(u,v)} \quad (2)$$

$$a_{coord} = \sum_{u=0}^W \sum_{v=0}^H M_{(u,v)} V_{coord(u,v)} \quad (3)$$

where H and W represent the unified height and width, respectively, of K , M , and V . (u, v) represents the coordinates at each representations. This attention module can determine the attention target by utilizing different Q s, which can be generated using various methods. The proposed model utilizes the internal states of the motion prediction module, which will be discussed later. The attention module also can be extended to multi-head attention. The outputs of each attention head are concatenated and denoted as A_{feat} and A_{coord} in hereafter.

C. Motion predictor module

This module (Fig. 2(c)) integrates data of three modalities, which are attention features A_{feat}^t , coordinates A_{coord}^t , and joint angles i_{joint}^t , and predicts each value at the next time step. The predicted joint angles \hat{o}_{joint}^{t+1} are utilized for motion generation, and the predicted attention values \hat{A}_{feat}^{t+1} and \hat{A}_{coord}^{t+1} are utilized as supportive data for training the entire model. The module is a layered structure composed of four units of LSTMs. Three LSTMs are lower-layered “modal LSTMs”, that predict future values of individual modalities. The remaining is an upper-layered “shared LSTM”, which integrates the internal states of the modal LSTMs and redistributes to share the states of different modalities. This layered structure is inspired by the characteristics of human cognitive activity, where information on visual features, positions and motions does not interfere within the working memory [28], [29]. h denotes the hidden states of each LSTMs.

$$\begin{cases} \hat{A}_{feat}^{t+1}, h_{feat}^t = LSTM_{feat}(A_{feat}^t, h_{feat}^{t-1}, h_{shared}^{t-1}) \\ \hat{A}_{coord}^{t+1}, h_{coord}^t = LSTM_{coord}(A_{coord}^t, h_{coord}^{t-1}, h_{shared}^{t-1}) \\ \hat{o}_{joint}^{t+1}, h_{joint}^t = LSTM_{joint}(i_{joint}^t, h_{joint}^{t-1}, h_{shared}^{t-1}) \end{cases} \quad (4)$$

$$\begin{cases} h_{shared}^t = LSTM_{shared}(h_{modal}^{t-1}, h_{shared}^{t-1}) \\ h_{modal}^{t-1} = Concatenate(h_{feat}^{t-1}, h_{coord}^{t-1}, h_{joint}^{t-1}) \end{cases} \quad (5)$$

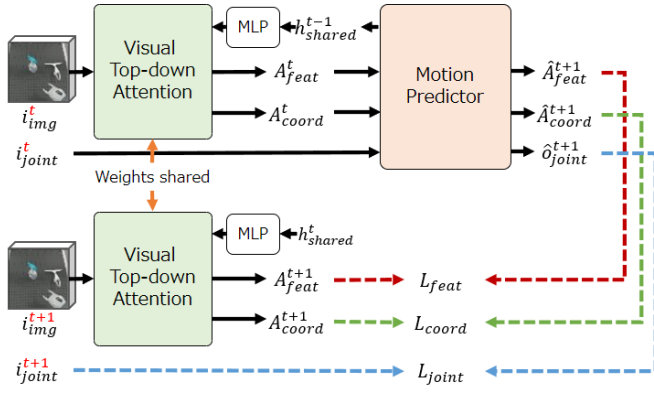


Fig. 3. Process of bi-directional loss. The loss of attention values predicted by the motion predictor module is computed with those predicted by the attention module using actual future images. Best viewed in color.

D. Query generation based on active feedback

In this model, the query vector for top-down attention is generated based on active feedback data from the motion predictor module (Fig. 2(b)). Concretely, the previous internal states of the shared LSTM h_{shared} are converted to a query vector with multilayer perceptrons (MLPs). As the shared LSTM integrates data of all modalities, we considered that the body and the environmental information are structured within. Therefore, the generated Q s are expected to acquire attention for suitable targets at each time step by considering the situation during task execution. On the initial time step, the Q was generated from a zero vector.

E. Bi-directional Loss

The proposed model is trained by optimizing it to minimize the error L , which is a weighted sum of future visuomotor prediction errors of modal LSTMs: L_{feat} , L_{coord} , and L_{joint} ; the applied weights are α_{feat} , α_{coord} , α_{joint} respectively. Minimizing the joint error (L_{joint}) leads to precise motion prediction, while minimizing the attention errors (L_{feat} and L_{coord}) leads to better recognition of the environment. However in the proposed model, the ground truth values of attention outputs do not exist. Therefore, this model employs a temporally bi-directional loss function, inspired by [30], which computes errors with self-simulated future values instead of ground-truth values. As Fig. 3 shows, future attention outputs predicted by LSTMs \hat{A}_{feat}^{t+1} and \hat{A}_{coord}^{t+1} , are compared with A_{feat}^{t+1} and A_{coord}^{t+1} . The comparison targets are predicted by a weight shared visual attention module, which is input the actual future image i_{img}^{t+1} in the dataset. This method is memory efficient compared to previous methods [7], [14], [8], that compute loss of reconstructed images with actual future images. The bi-directional loss not only eliminates redundant image reconstructions, but also induce the visual attention and motion prediction modules to predict attention points that are mutually consistent. In addition, this supports the layered LSTM to structure representations for active feedback, that better consider temporal context of visual data. Mean squared error (MSE) was used to compute the error of each prediction.

$$\begin{cases} L = \alpha_{feat}L_{feat} + \alpha_{coord}L_{coord} + \alpha_{joint}L_{joint} \\ L_{feat} = MSE(\hat{A}_{feat}^{t+1}, A_{feat}^{t+1}) \\ L_{coord} = MSE(\hat{A}_{coord}^{t+1}, A_{coord}^{t+1}) \\ L_{joint} = MSE(\hat{o}_{joint}^{t+1}, i_{joint}^{t+1}) \end{cases} \quad (6)$$

IV. EXPERIMENTS

A. Environmental setup

Fig. 5(a) displays the environmental setup of the experiment. The robot is ABB IRB 14000 YuMi, which is a dual-arm robot with each arm having seven degrees of freedom, and a gripper is installed. The camera on the robot is an Intel RealSense D435 RGBD camera (depth images were not used in this experiment). A white squeezeee was used as a tool and a spray bottle as the target object of interaction.

B. Task settings

The robot tool-use task was designed to induce active changes of attention targets. As Fig. 4 shows, the overall goal of the task is to pick the spray bottle object. However, different motions are performed depending on the position of the spray bottle. The robot directly picks the spray bottle with a gripper if it is placed nearby, whereas the robot drags the spray bottle with a tool before picking if it is placed at a distance. Hence, feature extraction of different visual targets are necessary in each motion: spray bottle and gripper for the picking motion, and spray bottle and tool data for the dragging motion. This experiment was also designed to be analogous to the task in which tool-body assimilation was observed in Japanese macaques [22].

C. Training configurations

The model is trained on a dataset which consists of sequence data of camera images and joint angles (including gripper states) during the above-mentioned motions. Twelve sequences of each picking, dragging, and consecutive dragging-picking motion were collected; the length are 60, 60, and 120 timesteps, respectively. The object was placed at four different positions of close and distant range, and the tool was placed at four different positions as well.

The model was not only trained to learn the motion data, but also to self-determine which type of motion to generate, depending on the given situation. We expect that such a training induces the model to actively modify the attention targets when transitioning to different states. For training, the internal states of all LSTMs were restricted to match the initial/neutral state to enable smooth transition between motions, as in [31].

In the experiment, FCN_1 and FCN_2 were 3 layer FCNs, with $filters = \{30, 30, q_{dim} \times N\}$, $kernel = 3 \times 3$, and $stride = 2$. The model was set with $k_{dim} = q_{dim} = 10$ and $v_{dim} = 10$. The number of attention heads is $N = 4$, in reference to the average number of features a human can hold in the visual working memory. The MLP of active feedback consists of four fully connected layers, with

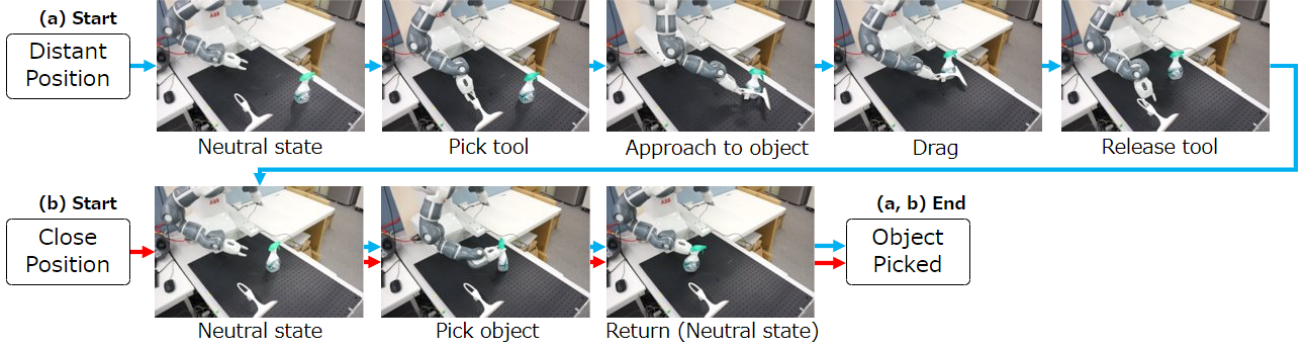
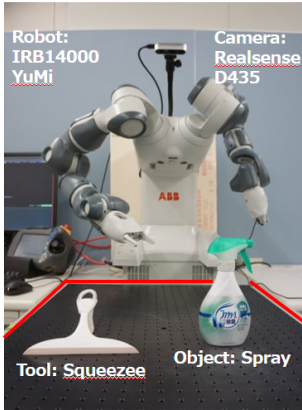


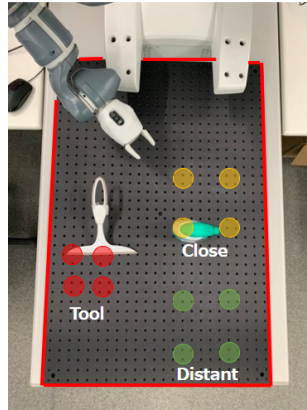
Fig. 4. Overall task flow of the trained motions. The objective is to pick the object. (a) When the object is placed at a distant position, the robot drags the object with a tool and then picks it up with the gripper. (b) When the object is placed nearby, the robot directly picks up the object with the gripper.

TABLE I
MOTION SUCCESS RATE UNDER DIFFERENT CONDITIONS

Motion Type	Proposed Model	Existing Models		Ablation Studies		
	Active + Layered	Vanilla FCN	FCN Attention	Active + Single	Passive + Layered	Passive + Single
Picking (close object)	27/30	0/30	3/30	0/30	0/30	0/30
Dragging (distant object)	30/30	20/30	22/30	22/30	15/30	9/30
Consecutive	26/30	0/30	3/30	0/30	0/30	0/30



(a) Environmental Setups



(b) Dataset Configurations

Fig. 5. Environmental setup of the experiment. (a) Hardware, tool, and object viewed from the front. (b) Positions where the tool and object were placed in the training data. Red indicates tool positions, yellow indicates close object positions and green indicates distant object positions

$nodes = \{300, 100, 60, q_{dim} \times N\}$. The shared and modal LSTMs were $nodes = 20$ and $nodes = 30$ respectively. The loss weights were $\alpha_{feat} = 0.001$, $\alpha_{coord} = 0.0001$, and $\alpha_{joint} = 0.9$. The model was trained by an ADAM optimizer with learning rate of 0.001, batch size 5, for 15000 epochs.

V. RESULTS AND DISCUSSION

A. Predicted motion and attention

Table I presents the motion success rate of the proposed model, which uses an “active” visual attention module and a “layered” LSTM motion predictor module. The success rate was measured for picking, dragging, and consecutive motions with 30 trials each, where the object and tool were placed at untrained positions. The motions were considered to have succeeded if the spray bottle was manipulated as expected. The results showed high precision for all motions,

and the model succeeded in precisely generating motions of the corresponding types. In an additional experiment, the model was presented with an unexpected situation, where the experimenter relocates the object to a distant position immediately after the model completed the dragging motion. The model handled this situation by regenerating the dragging motion instead of transitioning to the picking motion, which suggests that the model successfully learned to determine the motion based on the object location; more details are shown in the video.

Fig. 6 shows the four predicted attention points during consecutive dragging-picking motions, all of which stably acquired attention for different targets. Specifically, two among the four continuously acquired attention for the same targets, while the other two acquired attention for different targets during different motions. Table II summarizes the relationship between the targets of each four attention heads and the type of predicting motions. While attention #0 and #2 consistently directed attention to the same targets, attention #1 and #3 directed to visually dissimilar targets. However, considering the relation with the corresponding motions, the information extracted from such targets can be interpreted to have similar roles: the information extracted from attention #1 can be interpreted as the end-effector data, and that from attention #3 as supportive data. In this regard, we consider #1 and #3 to have acquired consistent role-based attention, in contrast to #0 and #2, which are conventional appearance-based attentions [18], [19], [20]. The existence of role-based attention suggests that the model actively modified the attention targets by considering the current situation that are fed back from the shared LSTM.

B. Comparison with existing models

The proposed model was compared to two existing robot motion prediction models. The models are similarly structured

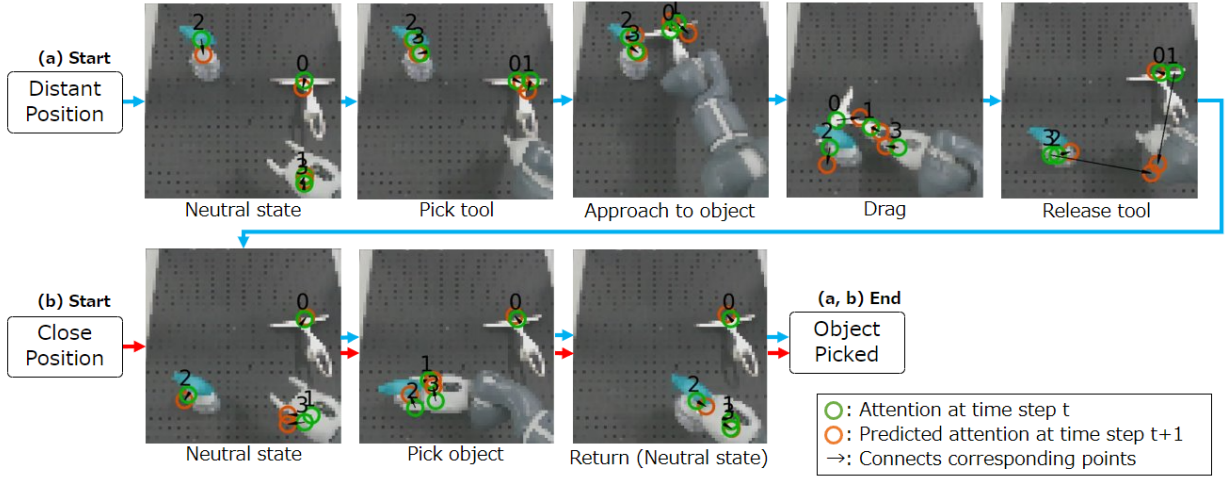


Fig. 6. Behavior of predicted attention points during consecutive dragging-picking motions. Attention #0 and #2 are appearance-based attentions, that constantly acquire attention for fixed targets. Attention #1 and #3 are role-based attentions that shift between targets based on a coherent role.

TABLE II
RELATIONSHIP BETWEEN ATTENTION TARGETS AND MOTIONS

Attention Head Index	Neutral/Picking (Object: Close)	Dragging (Object: Distant)
0	Tool	Tool
1	Gripper	Tool
2	Object	Object
3	Gripper	Object

with two modules, but with different vision models: (1) “Vanilla FCN” model [7], [14], which uses vanilla FCNs to extract the feature of the whole image. (2) “FCN Attention” model, which directly predicts attention points image feature of FCN output [18], [8]. This model is “passive”, as it does not incorporate active feedback from a motion prediction module. The two models are trained to minimize motion prediction errors, along with future image prediction error as an auxiliary loss.

Table I lists the respective task success rates and Fig. 7 shows the predicted attention points and future images. The success rates of the two models were low compared to the proposed model, especially on tasks that involve object picking. This is because picking requires higher precision compared to dragging, since there is only little difference in width between an opened gripper and spray. Specifically, “vanilla FCN” model performed poor due to the misrecognition of object positions, which can be observed from the predicted image in Fig. 7 (a); the object was reconstructed at an irrelevant image area. “FCN Attention” model succeeded in acquiring necessary attentions (gripper, tool, and object), and to generate appropriate motions at untaught situations. However, the model tended to perform picking at positions where the motion prediction module expected the object to be, rather than the actual positions perceived by the vision modules (Fig. 7(b)). More details are shown in the video. This is caused by the over-dependence on the auxiliary loss, in which the motion prediction is largely affected by the image prediction result. Such dependence also reduces the interpretability of the predicted future attention points, as shown in Fig. 7.

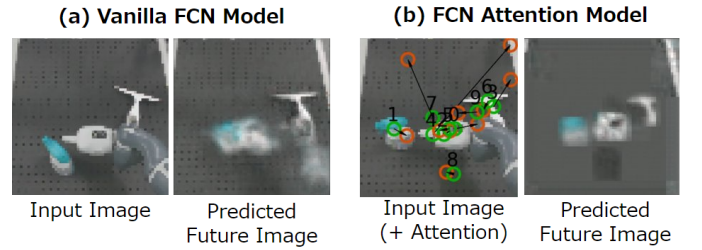


Fig. 7. Prediction results of existing models

C. Ablation study on proposed modules

To verify the functions of the two modules of the proposed model, an ablation study was conducted. Each module was modified and trained with all combinations of the following conditions: (1) use “Active” or “Passive” attention module and (2) use “Layered” or “Single” LSTM module; each conditions are explained in Section III-A. Among the four combinations, “Active + Layered” is the originally proposed structure. The modified models were trained and evaluated using the same dataset. As summarized in Table I, the performance substantially decreased with all modified structures. The following describes the predicted behavior of motions and attentions.

1) *Active + Single*: This model acquired attention for the necessary targets and showed active target modification during motion. However, the role-based attention showed inconsistent behaviors which tended to ignore the object after the dragging motion. Consequently, the model lost track of the object during the picking motion and failed to pick the object.

2) *Passive + Layered*: Although this model acquired appearance-based attention for the necessary targets, the model was vulnerable to appearance changes during motion. This caused the attention points to fluctuate between different targets unnecessarily, producing unstable robot motions.

3) *Passive + Single*: This model failed to acquire the necessary targets and showed vulnerability to appearance changes.

Accordingly, the results suggests the following feature of each structure. The “Active” attention structure enabled the model to actively modify attention targets and also be ro-

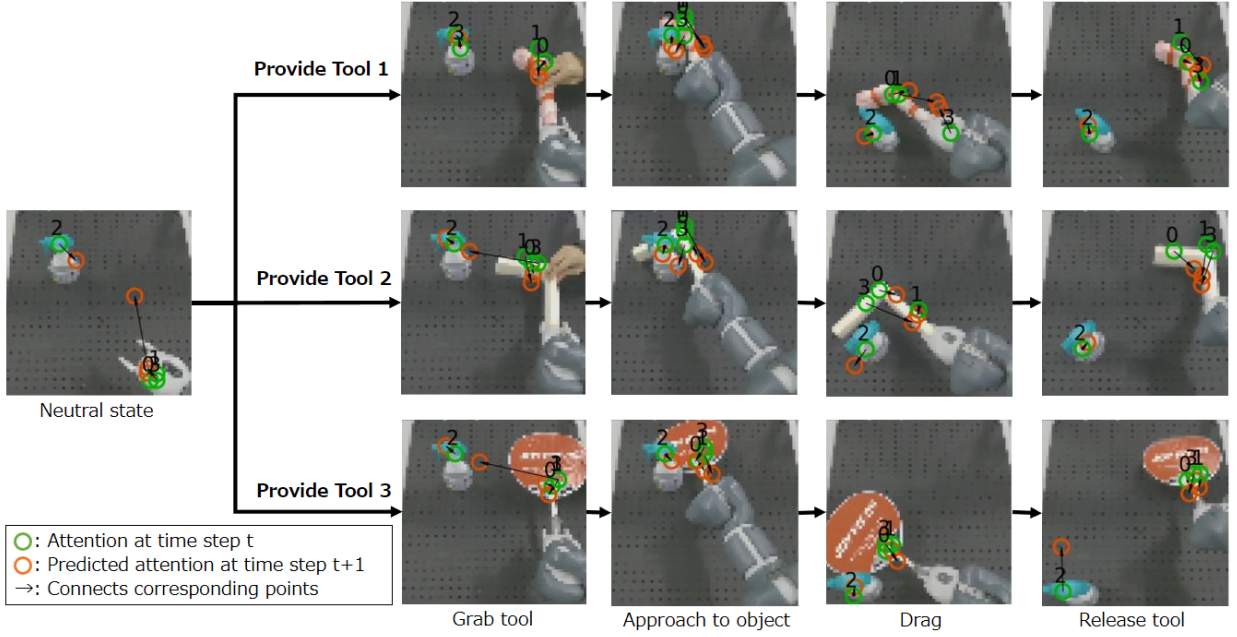


Fig. 8. Predicted motion and attention when provided with untrained types of tools.

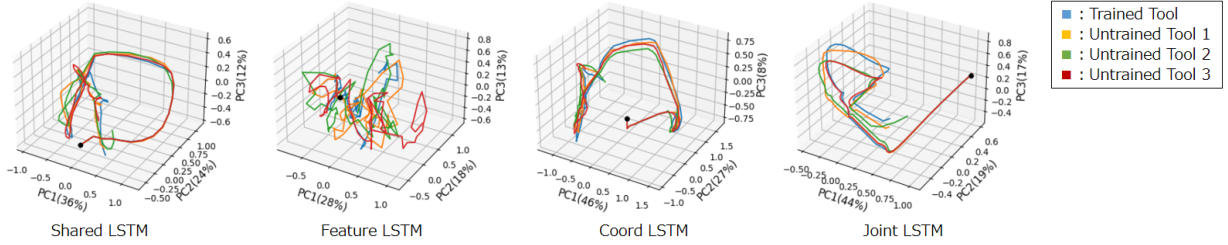


Fig. 9. Comparison of transitioning internal states of layered LSTMs. The data were collected while predicting the dragging motion using a trained tool and three untrained tools. The states are compressed to three dimensions using principle component analysis, where the colored lines represent the transition route of each internal states. The black dot represents the initial state.



Fig. 10. Sample results of predicted attention points when dragging with untrained tools. The end-effector attention (#1) ignored the trained tool throughout the motion.

bust to appearance changes. The “Layered” LSTM structure contributed to acquire role-based attentions that are coherent across different tasks.

D. Evaluation of tool-body assimilation

Considering the fact that the proposed model perceived both the tool and gripper as end-effectors (Fig. 6), we believe that the tool-body assimilation had emerged. For further analysis, an additional experiment was conducted to evaluate whether the model is capable of actively redefining the body schema (c.f. Section II-B). The model was evaluated by being presented with an untrained tool for performing dragging motions.

As Fig. 8 shows, the trained model generalized to use all the untrained tools and succeeded dragging the object. In addition, the previously mentioned role-based end-effector attention directed to the edged parts of the tools, where the robot actually hooked the object with. The attention on the untrained tools retained throughout the dragging motions, including those that had completely different appearances. Fig. 9 compares the transitioning internal states of the Layered LSTM while dragging using trained and untrained tools. The internal states of Shared, Coord, and Joint LSTMs transitioned similarly under all conditions, but slightly diverged after grasping the tools. This indicates that the model generated different motions for different tools, presumably based on the position of the predicted end-effector attention. In contrast, the states of the Feature LSTM diverged drastically after grabbing different tools; clear transitions are shown in video. This indicates that the attention module sustainably directed attention for each tool as the end-effector, with the knowledge that each tool is different. Since the model is not provided with any information of untrained tools, the first direction of the attention to the tools may have been an accident. However, the results indicate that the model actively modified the attention targets, since it ignored the original tool after grabbing an untrained tool (Fig. 10). This suggests that the model stored the feature of the

end-effector attention inside the internal states and actively updated the expected appearance of the tool. Such behavior of actively redefining the end-effector (or body schema) is analogous to that of Japanese macaques in Iriki's work [22], further suggesting the occurrence of tool-body assimilation.

VI. CONCLUSION

This paper proposed a novel real-time robot motion generation model, which consists of an active top-down attention module and a layered LSTM motion predictor module. Designating attention targets based on active feedback not only improved the stability of conventional appearance-based attention, but also acquired role-based attention that actively modifies attention targets according to the situation. When trained on a tool-use task, such role-based attention perceived the tool and the robot gripper as the same end-effector, which is analogous to the biological tool-body assimilation. Thus, the introduction of active visual attention extended the model's capability to perceive the environment flexibly and adaptively.

The proposed model is known to be capable of switching behaviors by control via external inputs. This feature enabled the model to handle camera movements during prediction in simulator environments, which we plan to apply to real-world robot tasks in the future work. Further, the current limitation in tool-use tasks is that generalizing to untrained tools is considered unstable because the initial recognition depends on an accidental behavior. This issue is also planned to be addressed in the future work.

REFERENCES

- [1] J. J. Gibson and L. Carmichael, *The senses considered as perceptual systems*. Houghton Mifflin Boston, 1966, vol. 2, no. 1.
- [2] S. Levine, C. Finn, T. Darrell, and P. Abbeel, "End-to-end training of deep visuomotor policies," *The Journal of Machine Learning Research*, vol. 17, no. 1, pp. 1334–1373, April 2016.
- [3] S. Gu, E. Holly, T. Lillicrap, and S. Levine, "Deep reinforcement learning for robotic manipulation with asynchronous off-policy updates," in *2017 IEEE international conference on robotics and automation (ICRA)*. IEEE, May 2017, pp. 3389–3396.
- [4] R. Yokoya, T. Ogata, J. Tani, K. Komatani, and H. G. Okuno, "Experience-based imitation using RNNPB," *Advanced Robotics*, vol. 21, no. 12, pp. 1351–1367, December 2007.
- [5] E. Uchibe and K. Doya, "Imitation learning based on entropy-regularized forward and inverse reinforcement learning," *ArXiv*, vol. abs/2008.07284, August 2020.
- [6] K. Takahashi, K. Kim, T. Ogata, and S. Sugano, "Tool-body assimilation model considering grasping motion through deep learning," *Robotics and Autonomous Systems*, vol. 91, pp. 115–127, May 2017.
- [7] H. Ito, K. Yamamoto, H. Mori, and T. Ogata, "Efficient multitask learning with an embodied predictive model for door opening and entry with whole-body control," *Science Robotics*, vol. 7, no. 65, p. eaax8177, April 2022.
- [8] H. Ichiwara, H. Ito, K. Yamamoto, H. Mori, and T. Ogata, "Spatial attention point network for deep-learning-based robust autonomous robot motion generation," *arXiv preprint arXiv:2103.01598*, March 2021.
- [9] R. Desimone and J. Duncan, "Neural mechanisms of selective visual attention," *Annual review of neuroscience*, vol. 18, no. 1, pp. 193–222, 1995.
- [10] G. D. Reynolds and A. C. Romano, "The development of attention systems and working memory in infancy," *Frontiers in Systems Neuroscience*, vol. 10, Mar 2016.
- [11] L. Itti, C. Koch, and E. Niebur, "A model of saliency-based visual attention for rapid scene analysis," *IEEE Transactions on pattern analysis and machine intelligence*, vol. 20, no. 11, pp. 1254–1259, December 1998.
- [12] S. Ren, K. He, R. Girshick, and J. Sun, "Faster r-cnn: Towards real-time object detection with region proposal networks," *Advances in neural information processing systems*, vol. 28, December 2015.
- [13] J. Redmon, S. Divvala, R. Girshick, and A. Farhadi, "You only look once: Unified, real-time object detection," in *Proceedings of the IEEE conference on computer vision and pattern recognition*, June 2016, pp. 779–788.
- [14] N. Saito, T. Ogata, S. Funabashi, H. Mori, and S. Sugano, "How to select and use tools? : Active perception of target objects using multimodal deep learning," *IEEE Robotics and Automation Letters*, vol. 6, no. 2, pp. 2517–2524, February 2021.
- [15] R. Liu, J. Lehman, P. Molino, F. Petroski Such, E. Frank, A. Sergeev, and J. Yosinski, "An intriguing failing of convolutional neural networks and the coordconv solution," *Advances in neural information processing systems*, vol. 31, July 2018.
- [16] A. Dosovitskiy, L. Beyer, A. Kolesnikov, D. Weissenborn, X. Zhai, T. Unterthiner, M. Dehghani, M. Minderer, G. Heigold, S. Gelly, J. Uszkoreit, and N. Houlsby, "An image is worth 16x16 words: Transformers for image recognition at scale," in *International Conference on Learning Representations*, May 2021.
- [17] N. Carion, F. Massa, G. Synnaeve, N. Usunier, A. Kirillov, and S. Zagoruyko, "End-to-end object detection with transformers," in *European conference on computer vision*. Springer, November 2020, pp. 213–229.
- [18] C. Finn, X. Y. Tan, Y. Duan, T. Darrell, S. Levine, and P. Abbeel, "Deep spatial autoencoders for visuomotor learning," in *2016 IEEE International Conference on Robotics and Automation (ICRA)*. IEEE, May 2016, pp. 512–519.
- [19] A. Zeng, P. Florence, J. Tompson, S. Welker, J. Chien, M. Attarian, T. Armstrong, I. Krasin, D. Duong, V. Sindhwani, and J. Lee, "Transporter networks: Rearranging the visual world for robotic manipulation," *Conference on Robot Learning (CoRL)*, October 2020.
- [20] H. Hiruma, H. Mori, and T. Ogata, "Guided visual attention model based on interactions between top-down and bottom-up information for robot pose prediction," February 2022.
- [21] D. Seita, P. Florence, J. Tompson, E. Coumans, V. Sindhwani, K. Goldberg, and A. Zeng, "Learning to rearrange deformable cables, fabrics, and bags with goal-conditioned transporter networks," in *2021 IEEE International Conference on Robotics and Automation (ICRA)*. IEEE, May 2021, pp. 4568–4575.
- [22] A. Maravita and A. Iriki, "Tools for the body (schema)," *Trends in cognitive sciences*, vol. 8, no. 2, pp. 79–86, February 2004.
- [23] M. Hikita, S. Fuke, M. Ogino, T. Minato, and M. Asada, "Visual attention by saliency leads cross-modal body representation," in *2008 7th IEEE International Conference on Development and Learning*. IEEE, September 2008, pp. 157–162.
- [24] C. Nabeshima, Y. Kuniyoshi, and M. Lungarella, "Towards a model for tool-body assimilation and adaptive tool-use," in *2007 IEEE 6th International Conference on Development and Learning*. IEEE, July 2007, pp. 288–293.
- [25] A. Stoytchev, "Behavior-grounded representation of tool affordances," in *Proceedings of the 2005 IEEE international conference on robotics and automation*. IEEE, April 2005, pp. 3060–3065.
- [26] M. Jung, T. Matsumoto, and J. Tani, "Goal-directed behavior under variational predictive coding: Dynamic organization of visual attention and working memory," in *2019 IEEE/RSJ International Conference on Intelligent Robots and Systems (IROS)*. IEEE, March 2019, pp. 1040–1047.
- [27] V. Prabhakaran, K. Narayanan, Z. Zhao, and J. Gabrieli, "Integration of diverse information in working memory within the frontal lobe," *Nature neuroscience*, vol. 3, no. 1, pp. 85–90, January 2000.
- [28] S. Della Sala, C. Gray, A. Baddeley, N. Allamano, and L. Wilson, "Pattern span: A tool for unwelding visuo-spatial memory," *Neuropsychologia*, vol. 37, no. 10, pp. 1189–1199, September 1999.
- [29] M. M. Smyth, N. A. Pearson, and L. R. Pendleton, "Movement and working memory: Patterns and positions in space," *The Quarterly Journal of Experimental Psychology Section A*, vol. 40, no. 3, pp. 497–514, August 1988.
- [30] S. Nishide, T. Ogata, J. Tani, K. Komatani, and H. G. Okuno, "Self-organization of dynamic object features based on bidirectional training," *Advanced Robotics*, vol. 23, no. 15, pp. 2035–2057, October 2009.
- [31] K. Kase, K. Suzuki, P.-C. Yang, H. Mori, and T. Ogata, "Put-in-box task generated from multiple discrete tasks by a humanoid robot using deep learning," in *2018 IEEE International Conference on Robotics and Automation (ICRA)*. IEEE, May 2018, pp. 6447–6452.